EUROPEAN JOURNAL OF PURE AND APPLIED MATHEMATICS
2026, Vol. 19, Issue 2, Article Number 7765
ISSN 1307-5543 – ejpam.com
Published by New York Business Global

An ODE Model of Th1/Th2 Immune Switching and Microglial Dynamics Reveals Rate-Dependent Thresholds Governing Neuronal Stability and Relapse

Haneen Hamam

Department of Mathematics, Jamoum University College, Umm Al-Qura University, Makkah 24320, Saudi Arabia

Abstract. In this study, we develop a mathematical model based on ordinary differential equations (ODEs) to investigate how immune responses influence neuronal stability and decline. The model focuses on interactions between Th1 and Th2 lymphocytes and their effects on microglial polarization, in which microglia can adopt either a pro-inflammatory (M1) or an anti-inflammatory (M2) phenotype. Through these interactions, immune activity can create conditions that either damage or protect neuronal populations. Our results indicate that when the immune response is dominated by Th1 activity, microglia tend to shift toward the M1 state, producing a pro-inflammatory environment that can progressively damage neurons. In contrast, stronger Th2 responses promote the M2 state, which supports anti-inflammatory and protective processes that help maintain neuronal stability. Sensitivity analysis further reveals that key parameters, including cytokine signaling rates and neuronal loss rates, play an important role in shaping these outcomes. Importantly, the model reveals a threshold-driven transition between neuronal stability and neurodegeneration, governed by the balance between pro-inflammatory and anti-inflammatory responses. This transition is associated with a change in the stability of the coexistence equilibrium, providing a mechanistic explanation for the shift between healthy and relapse states. By highlighting how immune balance regulates neuronal survival, the proposed model provides a quantitative framework for understanding how immune dysregulation may contribute to neuronal decline in neurodegenerative conditions such as Parkinson's disease. The analysis identifies parameter conditions that govern the transition from a stable neuronal state to neurodegeneration and highlights key factors that may influence neuronal relapse.

2020 Mathematics Subject Classifications: 34D20, 92C50, 37N25, 34C60

Key Words and Phrases: Th1/th2 immune switching, microglial dynamics, neuronal stability, neurodegeneration, Parkinson's disease

DOI: https://doi.org/10.29020/nybg.ejpam.v19i2.7765

Email addresses: hhhamam@uqu.edu.sa (H. Hamam)

1. Introduction

Parkinson's disease (PD) is a common neurodegenerative disorder that affects millions of people worldwide. It is primarily characterized by the progressive loss of dopaminergic neurons in the substantia nigra pars compacta, which ultimately leads to the motor symptoms associated with Parkinsonian conditions. Classical descriptions of PD pathophysiology emphasize mechanisms such as mitochondrial dysfunction and the aggregation of α-synuclein proteins [1–4]. However, increasing evidence suggests that immune responses and neuroinflammatory processes may also play an important role in shaping the neuronal environment and influencing neuronal survival [5, 6]. Recent studies increasingly suggest that neuroinflammation is not merely a secondary consequence of neurodegeneration, but an important contributor to disease progression through sustained immune activation and neuronal stress [7].

Among immune cells, $CD4^+$ T-helper lymphocytes are commonly divided into two main subsets, Th1 and Th2, which perform opposing immunological roles. Th1 cells promote inflammatory activity by secreting cytokines such as interferon-gamma (IFN-γ) and tumor necrosis factor-alpha (TNF-α). These signals can stimulate microglia to adopt the M1 phenotype, a pro-inflammatory state characterized by the release of reactive oxygen species, nitric oxide, and other inflammatory mediators that may contribute to neuronal stress and damage [8, 9]. In contrast, Th2 cells produce anti-inflammatory cytokines, including interleukin-4 (IL-4) and interleukin-13 (IL-13), which encourage microglial polarization toward the M2 phenotype. This state is generally associated with regulatory and protective functions that may support neuronal stability and tissue repair [10]. Emerging evidence suggests that microglia exhibit dynamic and context-dependent behavior, shifting between neuroprotective and neurotoxic states depending on the surrounding immune signals [11].(see Figure 1).

Several clinical observations indicate that immune regulation in Parkinson's disease may shift toward a predominance of Th1 responses over Th2 activity. This imbalance creates a persistent pro-inflammatory environment and has been associated with worsening motor symptoms and faster disease progression [12, 13]. Such findings suggest that the balance between pro-inflammatory and anti-inflammatory immune pathways may play an important role in determining the fate of dopaminergic neurons.

Given that the progressive loss of dopaminergic neurons represents a defining pathological feature of Parkinson's disease, the present study focuses on neuronal dynamics as the central component of the system. In particular, we investigate how the balance between adaptive immune responses, represented by Th1 and Th2 lymphocytes, influences microglial polarization into the pro-inflammatory (M1) and anti-inflammatory (M2) states and consequently affects neuronal stability or decline. By examining these coupled immune–neuronal interactions, the model aims to distinguish conditions associated with neuronal stability from those leading to progressive neuronal deterioration. In this context, mathematical modeling—particularly systems based on nonlinear ordinary differential equations—has emerged as a powerful framework for capturing complex immune–neuronal dynamics and identifying threshold-driven transitions in disease progression.

To better understand the complex interactions underlying neurodegeneration, several mathematical models have been developed to describe the dynamic relationships between neuronal loss, inflammation, and immune signaling in Parkinson's disease [14–19]. These models have provided valuable insights into disease mechanisms and have been used to evaluate potential therapeutic strategies.

Early work by Porenta et al. (1986) introduced a mathematical framework based on ordinary differential equations (ODEs) to describe dopamine feedback mechanisms in the basal ganglia [14]. More recently, Badrah and Al-Tuwairqi (2022) proposed a model capturing the interactions between neurons and microglia, demonstrating that system dynamics can shift between stable and destabilizing regimes depending on parameter values [15]. This framework was further extended through the incorporation of delay differential equations to account for time-dependent immune processes [16].

Despite these advances, most existing models primarily focus on neuronal dynamics or innate immune responses, with limited attention given to adaptive immune regulation. In particular, the interactions between T helper cell subtypes (Th1/Th2), microglial polarization (M1/M2), and their combined influence on neuronal behavior remain insufficiently explored.

To address this gap, the present study extends existing mathematical models by integrating adaptive immune responses with microglial dynamics and neuronal behavior. Specifically, the model incorporates the regulatory roles of Th1 and Th2 lymphocytes, their effects on microglial polarization, and the consequent impact on neuronal survival under both physiological and pathological conditions.

The analysis reveals the existence of parameter-besad threshold conditions, where small variations in key parameters can trigger a transition from a stable, healthy state to a neurodegenerative state characterized by sustained inflammation and neuronal loss. Furthermore, a local sensitivity analysis is conducted to identify the most influential parameters governing neuronal outcomes, providing deeper insight into the mechanisms driving disease progression. These findings are consistent with patterns observed in neurodegenerative disorders such as Parkinson's disease.

Accordingly, this study aims to develop a simplified yet biologically relevant ODE-based model linking Th1/Th2 dynamics to neuronal outcomes, with a particular focus on threshold-driven transitions between health and degeneration.

The remainder of this paper is organized as follows. In section 2, we present the mathematical model and describe the assumptions underlying its formulation. Section 3 is devoted to the analysis of the model under different conditions. In section 3.1, we investigate the steady-state points of the system and examine their stability. In addition, subsection 3.2 presents numerical simulations to further illustrate the dynamical behavior of the system. Subsection 3.3 provides a sensitivity analysis to assess how variations in key parameters influence neuronal dynamics over time scales of approximately 10 and 100 days. Finally, Section 4 concludes the paper with a summary of the main findings and their implications for neuronal stability and relapse.

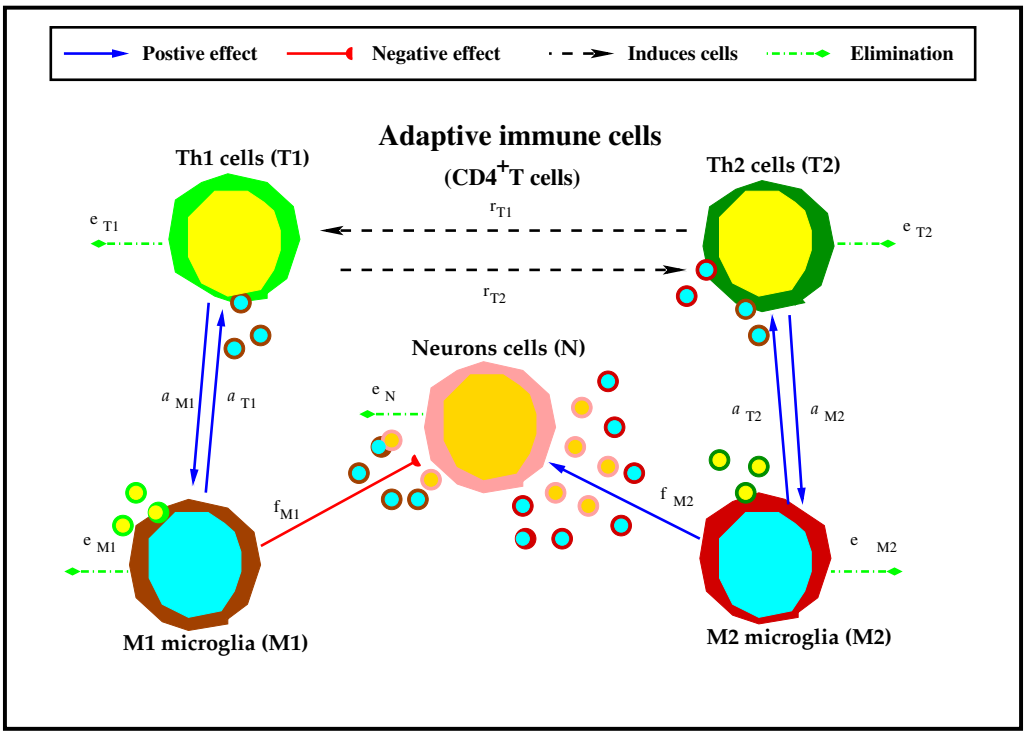

Figure 1: The schematic representation of the crosstalk between adaptive immune cells and microglia illustrates key signaling pathways and cellular interactions involved in central nervous system immune responses.

2. A Dynamic ODE Model of Adaptive Immune–Microglia Interactions Governing Neuronal Stability and Relapse

The proposed model focuses on five key populations that represent the core components of the immune-neuronal interaction: Th1 cells ($T1$), Th2 cells ($T2$), pro-inflammatory microglia ($M1$), anti-inflammatory microglia ($M2$), and the neuronal population (N). These components interact dynamically and are described by a system of ordinary differential equations (ODEs) that capture their regulatory and feedback relationships (see Figure 1).

The model is intentionally kept simple, following the principle of parsimony in mathematical biology, to highlight the essential dynamics without unnecessary complexity [20]. Although additional biological factors such as cytokines, dopaminergic pathways, and other molecular mediators play important roles in neurodegenerative processes, their effects are incorporated implicitly within the model parameters. In particular, cytokine signaling is reflected through interaction terms and transition rates between immune populations, while dopaminergic dysfunction is represented through its overall impact on neuronal survival and immune modulation.

The main objective of this study is to understand the switching behavior between pro-inflammatory (Th1-dominated) and anti-inflammatory (Th2-dominated) immune responses, and how this balance influences neuronal stability or relapse. This switching

mechanism is governed by the relative transition rates between Th1 and Th2 phenotypes, modeled through the parameters r_{T1} and r_{T2}. The model reveals the presence of a parameter-besad threshold that separates a stable, healthy neuronal state from a degenerative one, indicating that the overall system behavior is primarily driven by the balance between competing immune responses.

These findings are consistent with observations in neurodegenerative diseases, including Parkinson's disease, where immune imbalance, microglial activation, and chronic inflammation contribute to progressive neuronal loss [13, 21].

$$\frac{dT1}{dt} = p_{T1}T1M1\Big(1 - \frac{T1+T2}{\beta_T}\Big) - e_{T1}T1 - r_{T2}T1 + r_{T1}T2 + a_{T1}M1T1, \tag{1a}$$

$$\frac{dT2}{dt} = p_{T2}T2M2\Big(1 - \frac{T1+T2}{\beta_T}\Big) - e_{T2}T2 + r_{T2}T1 - r_{T1}T2 + a_{T2}M2T2, \tag{1b}$$

$$\frac{dM1}{dt} = p_{M1}T1M1\Big(1 - \frac{M1+M2}{\beta_M}\Big) - e_{M1}M1 + a_{M1}T1M1, \tag{1c}$$

$$\frac{dM2}{dt} = p_{M2}T2M2\Big(1 - \frac{M1+M2}{\beta_M}\Big) - e_{M2}M2 + a_{M2}T2M2, \tag{1d}$$

$$\frac{dN}{dt} = p_N N\Big(1 - \frac{N}{\beta_N}\Big) - e_N N + f_{M2}M2N - f_{M1}M1N. \tag{1e}$$

In the following, we describe in detail the terms that appear in model (1).

- Equation (1a) describes the population dynamics of Th1 cells. The term $p_{T1}T1M1\left(1 - \frac{T1+T2}{\beta_T}\right)$ represents proliferation of Th1 cells driven by pro-inflammatory cytokines, where p_{T1} is the intrinsic proliferation rate of Th1 cells. This proliferation is driven by pro-inflammatory cytokines such as IL-12 and TNF-α, which are produced by activated microglia and contribute to inflammatory immune responses in the central nervous system [22]. Although both terms share a similar multiplicative structure involving $M1T1$, they represent distinct mechanisms: the proliferation term captures density-dependent population growth constrained by carrying capacity, whereas the activation term describes cytokine-driven functional amplification without imposing additional resource limitations.The growth is limited by a carrying capacity β_T. In contrast, the term $a_{T1}M_1T_1$ represents cytokine-mediated activation of existing Th1 cells [8]. Unlike the logistic proliferation term, this mechanism does not introduce density-dependent constraints and does not imply independent population growth, but rather reflects the amplification of the activity and expansion rate of already present Th1 cells. Thus, proliferation corresponds to population growth through cell division under resource limitation, whereas activation represents cytokine-driven enhancement of the existing immune response without introducing an additional carrying capacity constraint. The transition between Th1 and Th2 phenotypes is modeled using constant rates r_{T1} and r_{T2}, following simplified representations of immune plasticity [23, 24]. These rates should be interpreted as averaged switching effects rather than detailed cytokine-regulated processes. Finally, Th1 cells undergo natural decay at rate e_{T1} [25, 26].

- Equation (1b) describes the population dynamics of Th2 cells. The term $p_{T2}T_2M_2\left(1-\frac{T_1+T_2}{\beta_T}\right)$ represents logistic proliferation of Th2 cells driven by anti-inflammatory cytokines, where p_{T2} is the intrinsic proliferation rate. This proliferation is mediated by cytokines such as IL-4 and IL-13, which promote Th2 differentiation and are associated with alternative (M2) activation of microglia/macrophages [8, 27]. The logistic formulation captures density-dependent growth limited by the carrying capacity β_T.In addition to proliferation, the term $a_{T2}M_2T_2$ represents cytokine-mediated activation and amplification of the existing Th2 population. Unlike the logistic proliferation term, this mechanism does not impose density-dependent constraints and does not represent de novo generation of Th2 cells. Instead, it captures the enhancement of the Th2 response through cytokine signaling. The transition between Th2 and Th1 phenotypes is modeled using constant rates r_{T1} (Th2 $\rightarrow$ Th1) and r_{T2} (Th1 $\rightarrow$ Th2), following simplified representations of immune plasticity [23, 24]. These rates are interpreted as averaged switching effects rather than detailed cytokine-regulated processes. Finally, Th2 cells undergo natural decay at a rate e_{T2} [25, 26].

- Equation (1c) describes the dynamics of M1 microglial cells. The term $p_{M1}T_1M_1\left(1-\frac{M_1+M_2}{\beta_M}\right)$ represents logistic proliferation of M1 cells driven by pro-inflammatory signals associated with Th1 responses, where p_{M1} is the effective proliferation rate. These signals include cytokines such as IFN-γ, TNF-α, and IL-12, which are known to promote classical (M1) activation of microglia/macrophages [28]. The logistic term captures density-dependent growth limited by the carrying capacity β_M. In addition to proliferation, the term $a_{M1}T_1M_1$ represents cytokine-mediated activation and amplification of the existing M1 population under Th1-associated signaling. Unlike the logistic proliferation term, this mechanism does not impose density-dependent constraints and reflects enhancement of the pro-inflammatory response rather than de novo generation of M1 cells [29, 30].Finally, M1 cells undergo natural decay at rate e_{M1} [31].

- Equation (1d) describes the dynamics of M2 microglial cells. The term $p_{M2}T_2M_2\left(1-\frac{M_1+M_2}{\beta_M}\right)$ represents logistic proliferation of M2 cells driven by anti-inflammatory signals associated with Th2 responses, where p_{M2} is the effective proliferation rate. These signals include cytokines such as IL-4 and IL-13, which are known to promote alternative (M2) activation of microglia/macrophages [32]. The logistic formulation captures density-dependent growth limited by the carrying capacity β_M. In addition to proliferation, the term $a_{M2}T_2M_2$ represents cytokine-mediated activation and amplification of the existing M2 population under Th2-associated signaling. Unlike the logistic proliferation term, this mechanism does not impose density-dependent constraints and reflects enhancement of the anti-inflammatory response rather than de novo generation of M2 cells [29, 32]. Finally, M2 cells undergo natural decay at rate e_{M2} [31].

- The dynamics of the neuronal population are governed by Eq. (1e). Although most mature neurons are terminally differentiated, experimental studies have shown that adult neurogenesis can occur under specific physiological or environmental conditions, particularly in restricted regions such as the hippocampus and the subventricular zone [33]. In this model, the variable N is interpreted as an effective measure of neuronal viability or functional integrity, rather than strictly representing the number of newly generated neurons. Accordingly, a logistic growth term $p_N N\left(1-\frac{N}{\beta_N}\right)$ is used as a phenomenological approximation to capture the balance between limited regenerative or compensatory mechanisms and resource constraints, where p_N is the effective recovery rate and β_N represents the maximal sustainable neuronal level. In addition to intrinsic dynamics, neuronal survival is modulated by microglial activity. Anti-inflammatory M2 microglia promote neuronal survival through neuroprotective and trophic effects [28, 32, 34], which is represented by the term $f_{M2}M2N$. In contrast, pro-inflammatory M1 microglia contribute to neuronal damage via the release of inflammatory mediators and neurotoxic factors [28, 32], modeled by the damage term $f_{M1}M1N$. Finally, neuronal loss is accounted for by a natural decay term at rate e_N [35].

All parameters associated with model (1) are listed in Table A. In this study, the parameters are assumed to remain constant over time in order to better understand the intrinsic behavior of the system. Allowing parameters to vary with time, especially those related to switching rates or cytokine-driven interactions, could introduce additional complexity, such as time-dependent thresholds or delayed responses. However, exploring such effects is beyond the scope of the present work and is left for future research.

3. Results

In this study, we investigate model (1) by analyzing its steady-state equilibria and examining their stability conditions. The equilibrium analysis describes the long-term behavior of the system and reveals its underlying stability structure. The results identify two biologically meaningful regimes: a healthy neuronal state and a neurodegenerative regime. Numerical simulations illustrate the system dynamics and reveal a threshold mechanism governing the transition from neuronal stability to neuronal decline. Finally, a local sensitivity analysis is performed to determine the most influential parameters affecting the system dynamics.

3.1. Steady states and stability

The equilibrium points of system (1) are obtained by solving

$$\frac{dT1}{dt}=0,\quad \frac{dT2}{dt}=0,\quad \frac{dM1}{dt}=0,\quad \frac{dM2}{dt}=0,\quad \frac{dN}{dt}=0.$$

From these equations, several biologically meaningful equilibrium states can be identified depending on which populations persist in the system. In particular, the following

equilibrium states are considered in this study:

(i) No immune and neuronal cells steady state: $E_0 = (0, 0, 0, 0, 0)$. The non-zero equilibrium state, determined by the baseline parameters in Table A, is classified as *dynamically unstable*. More generally, the stability properties of this state are analyzed in Proposition 1.

(ii) Immune-free steady state corresponding to the absence of both pro-inflammatory (Th1, M1) and anti-inflammatory (Th2, M2) immune responses, with only neuronal cells present: $E_1 = (0, 0, 0, 0, N^*)$

$$N^* = (p_N - e_N)\frac{\beta_N}{p_N} \qquad \text{if } p_N > e_N.$$

Linearization around E_1 shows that, under the baseline parameter values listed in Table A, this equilibrium is locally asymptotically stable whenever $p_N > e_N$. However, from a biological perspective, this state is not physiologically realistic, as the complete absence of immune activity does not occur under normal conditions. Therefore, E_1 should be interpreted as a theoretical reference state rather than a biologically attainable healthy state.

(iii) Coexistence equilibrium of pro-inflammatory (Th1, M1), anti-inflammatory (Th2, M2), and neuronal cells: $E_2 = (T1^*, T2^*, M1^*, M2^*, N^*)$. For biological feasibility, the coexistence equilibrium E_2 requires

$$T1^* > 0, \quad T2^* > 0, \quad M1^* > 0, \quad M2^* > 0, \quad N^* > 0.$$

The coexistence equilibrium E_2 is characterized by the following implicit system of algebraic equations:

$$T1^* = \frac{e_{M1}}{a_{M1} + p_{M1}\left(1 - \dfrac{M1^* + M2^*}{\beta_M}\right)}, \quad T2^* = \frac{e_{M2}}{a_{M2} + p_{M2}\left(1 - \dfrac{M1^* + M2^*}{\beta_M}\right)},$$

$$M1^* = \frac{e_{T1} + r_{T2} - r_{T1}\dfrac{T2^*}{T1^*}}{a_{T1} + p_{T1}\left(1 - \dfrac{T1^* + T2^*}{\beta_T}\right)}, \quad M2^* = \frac{e_{T2} + r_{T1} - r_{T2}\dfrac{T1^*}{T2^*}}{a_{T2} + p_{T2}\left(1 - \dfrac{T1^* + T2^*}{\beta_T}\right)},$$

$$N^* = \beta_N\left(1 - \frac{e_N - f_{M2}M2^* + f_{M1}M1^*}{p_N}\right).$$

Due to the nonlinear coupling between the state variables, these expressions do not yield an explicit closed-form solution. Instead, the equilibrium values are obtained numerically under the baseline parameter set given in Table A.

In general, the behavior near the coexistence equilibrium E_2 is influenced by the balance between pro- and anti-inflammatory responses. Numerical evaluation of

the Jacobian matrix at E_2 under the baseline parameter values given in Table A indicates that all eigenvalues have negative real parts, indicating that E_2 is locally asymptotically stable under these specific parameter conditions.

As will be illustrated in the following section 3.2.3, numerical simulations further reveal that this balance leads to a threshold-like behavior in the (r_{T1}, r_{T2}) parameter space.

3.2. Numerical results

To better understand how the immune system influences neuronal survival under different conditions, numerical simulations were performed using the parameter values listed in Table A. The model describes the populations of Th1 cells ($T1$), Th2 cells ($T2$), pro-inflammatory M1 microglia ($M1$), anti-inflammatory M2 microglia ($M2$), and neurons (N). Time is measured in days, and all populations are expressed in normalized units.

Because reliable biological data for the initial sizes of these immune populations are limited, moderate initial values were chosen to represent a reasonable baseline state before strong inflammation develops. Specifically, we set $T1(0) = 10$, $T2(0) = 8$, $M1(0) = 15$, $M2(0) = 10$, and $N(0) = 1000$. All initial conditions are given in dimensionless (normalized) units. The neuronal population starts at a higher level to reflect the abundance of healthy neurons before neurodegeneration, while immune populations are initialized at moderate levels corresponding to normal physiological activity.

The analysis focuses on the switching rates between Th1 and Th2 phenotypes, denoted by r_{T1} and r_{T2} (day^{-1}). By varying these parameters, we explore how changes in immune balance shape the interaction between pro-inflammatory (Th1, M1) and anti-inflammatory (Th2, M2) responses, and how this balance affects neuronal outcomes. Time evolution and phase-plane analysis help illustrate whether the system evolves toward a stable neuronal state or a neurodegenerative state characterized by sustained inflammation and neuronal loss.

The results indicate the presence of a threshold that governs the transition between neuronal stability and degeneration, where even small changes in the switching rates can significantly alter the system dynamics.

To construct the parameter-plane diagram, simulations were performed over a grid in the (r_{T1}, r_{T2}) parameter space. For each pair (r_{T1}, r_{T2}), the system was simulated until it reached a steady state. The classification of each point was based on the asymptotic value of the neuronal population $N(t)$:

- Healthy state: if $N(t \to \infty)$ converges to a high equilibrium level close to β_N,
- Relapse state: if $N(t \to \infty)$ converges to a low equilibrium level.

The threshold curve defines the boundary separating (a) the relapse regime and (b) the healthy regime in the parameter space, with (c) indicating the threshold-induced transition between neuronal stability and neuronal relapse.

3.2.1. (a) Reduced Neuronal Population in the Relapse State

We first consider the scenario in which the pro-inflammatory response dominates, leading to the instability of the coexistence equilibrium E_2. Figure 2 shows the temporal evolution of both immune and neuronal populations under this regime for $r_{T1} = 0.1$ and $r_{T2} = 0.01$. In the short-term dynamics (first 100 days, subfigure (i)), the neuronal population declines rapidly since $r_{T1} > r_{T2}$, meaning that the transition toward the Th1 phenotype is dominant. In other words, the conversion from Th2 to Th1 exceeds the reverse process. Consequently, Th1 and M1 populations quickly dominate, enhancing inflammatory activity and accelerating neuronal damage. Over the long term (subfigure (ii), up to 1000 days), neuronal levels continue to decrease and eventually reach critically low values. This reflects the sustained dominance of pro-inflammatory mechanisms, even in the presence of anti-inflammatory cells (Th2 and M2), whose neuroprotective role remains limited. Notably, even when $r_{T1} = r_{T2} = 0.1$, the neuronal population N still exhibits a declining trend.

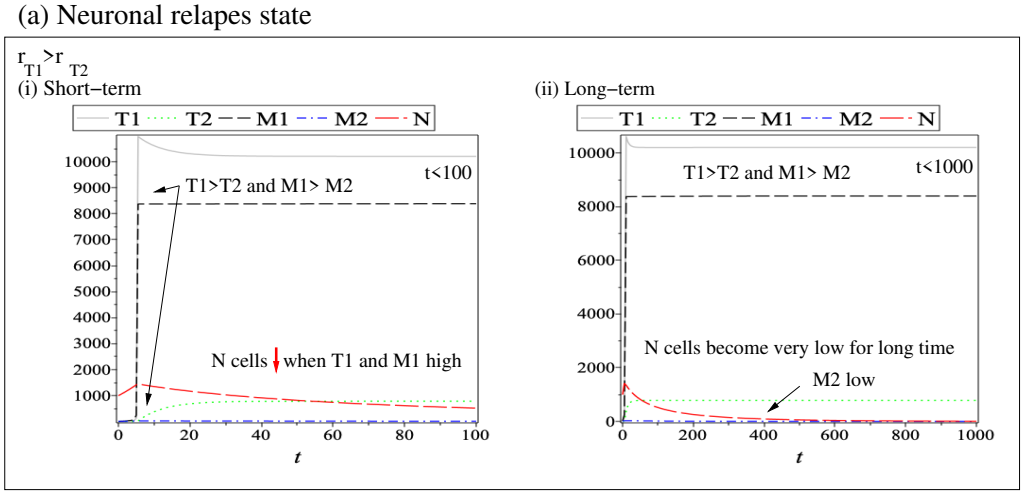

Figure 2: Dynamics of model (1) illustrating the system's evolution toward steady states under neurodegenerative conditions for $r_{T1} = 0.1$ and $r_{T2} = 0.01$ ($r_{T1} > r_{T2}$), corresponding to a pro-inflammatory dominant regime. Panels show: (i) short-term dynamics and (ii) long-term dynamics. The results indicate that increased Th1 activity promotes sustained microglial activation and leads to progressive neuronal decline before the system stabilizes at a lower neuronal equilibrium. All other parameter values are listed in Table A.

3.2.2. (b) Neuroprotective Immune Response (Healthy State)

In contrast, when the anti-inflammatory response dominates, the coexistence equilibrium E_2 remains stable, and the system converges to a healthy neuronal state. Figure 3 illustrates the model dynamics for the case $r_{T1} = 0.01 < r_{T2} = 0.1$, indicating that the transition toward the Th2 phenotype (from Th1 to Th2) dominates over the reverse process. In the short-term dynamics (for $t < 100$ days, panel (i)), the neuronal population increases due to the rapid induction of anti-inflammatory immune cells (Th2 and M2).

Panel (ii) shows the long-term behaviour (for $t < 1000$ days), where the neuronal population stabilizes and approaches the carrying capacity. This behavior reflects the dominance of Th2 and M2 cells, which promote neuroprotective and anti-inflammatory mechanisms, thereby supporting neuronal survival and maintaining system stability.

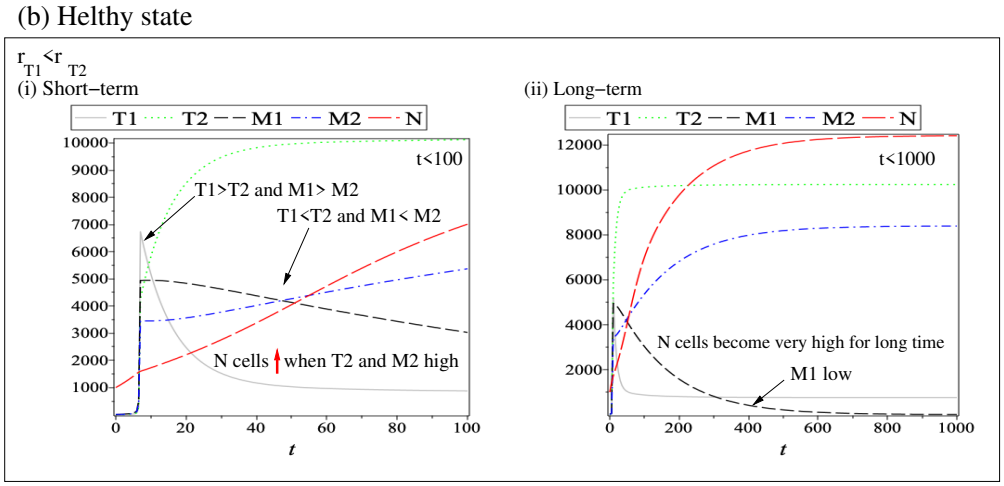

Figure 3: Dynamics of model (1) illustrating the system's approach to the healthy steady state under the condition $r_{T1} = 0.01$ and $r_{T2} = 0.1$ ($r_{T1} < r_{T2}$). The plots demonstrate: (i) short-term dynamics and (ii) long-term stabilization toward a non-pathological equilibrium. All other parameter values are provided in Table A.

These two regimes suggest the existence of a transition mechanism between neuronal stability and relapse, which we investigate in the following subsection.

3.2.3. (c) Threshold-Induced Transition Between Neuronal Stability and Neuronal Relapse

To better understand the system dynamics, we examine how variations in the switching parameters (r_{T1}, r_{T2}) influence neuronal outcomes. The results reveal the presence of a threshold separating neuronal stability from relapse, indicating that even small changes in these parameters can lead to noticeable shifts in system behavior.

Figure 4 illustrates the parameter-plane diagram in the (r_{T1}, r_{T2}) space, where different regions correspond to distinct neuronal outcomes. The threshold boundary was obtained through numerical simulations over a grid of parameter values. For each pair (r_{T1}, r_{T2}), the system was simulated until it reached a steady state, and the outcome was classified based on the long-term behavior of the neuronal population $N(t)$:

- Healthy state: if $N(t \to \infty)$ approaches a high equilibrium level close to β_N,
- Relapse state: if $N(t \to \infty)$ approaches a low equilibrium level.

The results indicate that this classification is largely determined by the ratio

$$\frac{r_{T1}}{r_{T2}} \approx 0.25, \tag{4}$$

which was identified numerically.

It is important to note that this threshold is not a universal constant, but depends on the underlying model parameters. In particular, variations in key parameters may shift the location of this boundary. Although the threshold was identified numerically, the sensitivity analysis indicates that variations in key parameters can influence the overall system behavior, which may consequently shift the approximate location of this transition boundary. From a dynamical systems perspective, this transition reflects a change in system behavior, where small variations in the ratio $\frac{r_{T1}}{r_{T2}}$ can lead to noticeable changes in the long-term neuronal outcome.

In particular,

$$\text{Relapse region} \quad \text{if} \quad \frac{r_{T1}}{r_{T2}} > 0.25, \tag{5}$$

$$\text{Threshold boundary} \quad \text{if} \quad \frac{r_{T1}}{r_{T2}} \approx 0.25, \tag{6}$$

$$\text{Healthy region} \quad \text{if} \quad \frac{r_{T1}}{r_{T2}} < 0.25. \tag{7}$$

This ratio reflects the balance between the two immune pathways: increasing r_{T1} shifts the system toward a pro-inflammatory Th1-dominated response, while increasing r_{T2} promotes the anti-inflammatory Th2 response. The threshold, therefore, marks the point at which pro-inflammatory activity begins to dominate, leading to neuronal decline. As shown in Figure 4, the blue region corresponds to relapse, whereas the red region represents the healthy state, with the green curve marking the boundary between these regimes.

These results are consistent with known immune–neuronal interactions, where sustained pro-inflammatory activity is associated with neuronal damage, while anti-inflammatory responses promote neuronal survival.

To illustrate the system behavior near this boundary, we examine the temporal dynamics at $\frac{r_{T1}}{r_{T2}} \approx 0.25$, as shown in Figure 5. Figure 5 illustrates the temporal evolution of the system under this condition, where a transition from a relapse state to a healthy state is observed. During the initial phase, the neuronal population N remains at low levels, reflecting a relapse condition driven by the dominance of pro-inflammatory components (Th1 and M1). In this regime, elevated Th1 activity promotes M1 polarization, leading to sustained inflammatory signaling and continuous neuronal damage. As time progresses, the system undergoes a gradual reorganization of the immune response, characterized by a decrease in Th1/M1 activity and a corresponding increase in Th2 and M2 populations. This shift reflects a phenotypic switching mechanism through which anti-inflammatory pathways progressively counterbalance and eventually overcome the pro-inflammatory response. A critical transition occurs when the system crosses an approximate threshold

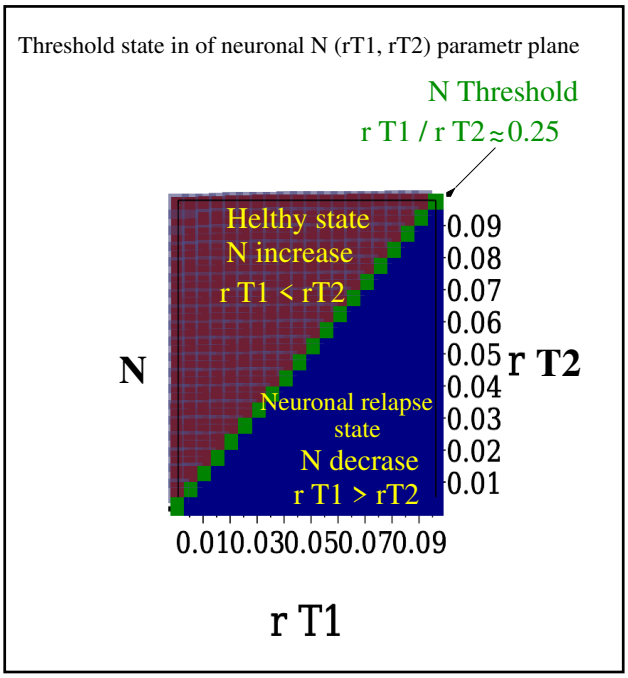

Figure 4: Dynamics of model (1) illustrating the threshold-induced transition between healthy and neuronal relapse states governed by the parameters r_{T1} and r_{T2}. Panel shows the parameter-plane diagram in the (r_{T1}, r_{T2}) space. The regions are classified based on the long-term behavior of the neuronal population $N(t)$: the red region corresponds to the healthy state, where $N(t)$ converges to a high stable equilibrium; the blue region represents the relapse state, where $N(t)$ declines to a low equilibrium; and the green curve denotes the threshold boundary separating these two regimes. All remaining parameter values are given in Table A.

threshold at which anti-inflammatory components become dominant. In the extended-time regime, this dominance is characterized by $T2 > T1$ and $M2 > M1$, resulting in the suppression of inflammatory damage and restoration of neuronal integrity. Consequently, the neuronal population recovers and asymptotically approaches a high, non-pathological equilibrium level. The regimes $\frac{r_{T1}}{r_{T2}} > 0.25$ and $\frac{r_{T1}}{r_{T2}} < 0.25$ are presented in sections 3.2.1 and 3.2.2, respectively, while the present case $\frac{r_{T1}}{r_{T2}} \approx 0.25$ represents the transition between them. Overall, these results indicate that neuronal outcomes are strongly governed by the balance between Th1 and Th2 dynamics, which directly affects the stability of the coexistence equilibrium E_2. This behavior is consistent with observations in neurodegenerative diseases, including Parkinson's disease, where immune imbalance plays a key role in progressive neuronal loss [13, 21].

3.3. Local sensitivity analysis

Sensitivity analysis was conducted because several parameter values in the model were not directly available in the literature and therefore had to be estimated. To evaluate the robustness of the model under parameter uncertainty, a local sensitivity analysis was performed. In this approach, each parameter S was varied over a broad range around

(c) Neuronal recovery under balanced transition rates $r_{T1}/ r_{T2} \simeq 0.25$

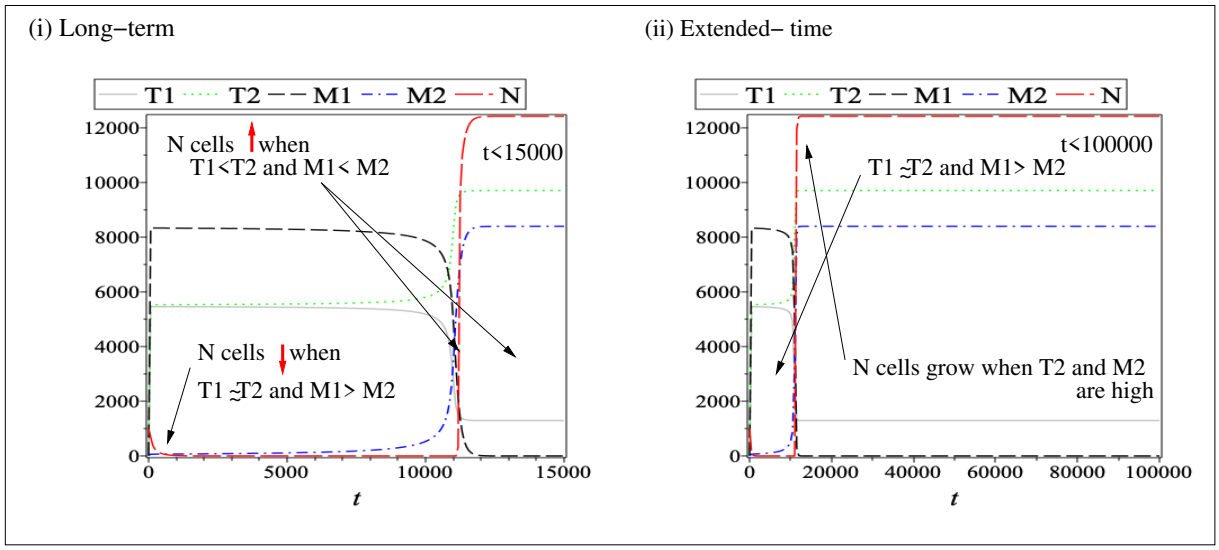

Figure 5: Dynamics of model (1) illustrating the system's transition from relapse to a healthy steady state under the condition $\frac{r_{T1}}{r_{T2}} \approx 0.25$ ($r_{T1} = 0.01 < r_{T2} = 0.04$). The plots show: (i) long-term dynamics and (ii) extended-time convergence toward a non-pathological equilibrium. All other parameter values are given in Table A.

its nominal value. Specifically, parameters were perturbed by $\pm 10\%$, representing small variations, and by $\pm 90\%$, representing larger deviations. The resulting relative change ratios are illustrated in Figure 6, allowing a direct comparison of parameter influence at three different time points: day 10, day 100, and day 1000.

To quantify the influence of parameter variations on the system dynamics, the relative sensitivity index was computed. For a given state variable $X(t)$ and parameter S, the sensitivity measure is defined as

$$G_S^X(t) = \frac{X(t,S) - X(t,S_0)}{X(t,S_0)},$$

where $X(t,S)$ represents the solution obtained after perturbing parameter S, and $X(t,S_0)$ denotes the baseline solution corresponding to the nominal parameter value S_0.

A local sensitivity analysis was performed to assess the effect of parameter variations on the system dynamics. This approach identifies the parameters that exert the strongest influence on system behavior, as well as those with only minor effects. Consequently, it provides insight into the robustness of the model predictions and highlights the key biological mechanisms governing immune interactions and neuronal dynamics.

Figure 6 illustrates the sensitivity of the neuronal population to immune-modulatory parameters, particularly those associated with microglial activity and T-helper cell dynamics. Panel (a) corresponds to day 10, while panels (b) and (c) represent days 100 and 1000, respectively.

The results show that increasing pro-inflammatory activity—driven by M1-like microglia proliferation (p_{M1}), Th1 cell proliferation (p_{T1}), and the neuronal elimination rate (e_N)—leads to a significant reduction in neuronal population levels, especially at early time points (day 10). In contrast, increasing anti-inflammatory activity through higher M2 microglia activation (a_{M2}) and Th2-related responses, together with decreasing Th1 proliferation (p_{T1}), results in an increase in neuronal cell levels.

Although the detrimental effects of pro-inflammatory factors are most pronounced at early stages, their impact becomes less significant at later time points (days 100 and 1000), indicating a shift in system sensitivity over time.

Furthermore, increasing the M2 microglia growth rate mediated by Th2 cells (a_{M2}), while decreasing the M1 microglia growth rate via Th1 cells (a_{M1}) and the proliferation rate of M1 microglia (p_{M1}), promotes a sustained increase in neuronal population levels across all time points. These findings emphasize the critical role of the balance between pro-inflammatory and anti-inflammatory mechanisms in regulating neuronal survival.

The results of the local sensitivity analysis are consistent with the threshold behavior observed in the model. In particular, the system is most sensitive to parameters that regulate the balance between pro-inflammatory (Th1/M1) and anti-inflammatory (Th2/M2) responses.

The parameter-besad threshold, defined by the ratio $\frac{r_{T1}}{r_{T2}} \approx 0.25$, indicates that neuronal outcomes depend on the relative dominance of these competing immune pathways. Parameters that promote pro-inflammatory activity, such as p_{T1} and p_{M1}, tend to drive the system toward relapse by enhancing Th1 cell activation and expansion, thereby strengthening the pro-inflammatory response. In contrast, increased M2 activation (a_{M2}) supports neuronal stability by reinforcing the anti-inflammatory response and counteracting pro-inflammatory effects.

These findings show that the most influential parameters are those that determine how close the system is to the threshold boundary. As a result, even small changes in these parameters can shift the system across the threshold, leading to a transition between neuronal stability and degeneration.

Overall, the sensitivity analysis not only identifies the key parameters but also provides a mechanistic explanation for the threshold-driven switching behavior. The results are consistent with known immune–neuronal interactions, where pro-inflammatory activity promotes neuronal damage and anti-inflammatory responses support neuronal survival. This agreement with biological expectations reinforces the validity and robustness of the proposed model.

4. Conclusion

The mathematical model developed in this study provides insight into how interactions between the immune system and the brain may influence the stability or relapse of neuronal populations. Our results suggest that when the immune response becomes dominated by Th1-associated cytokines (e.g., IFN-γ, TNF-α), microglia tend to adopt a pro-inflammatory M1 phenotype. In this state, the neural environment becomes increas-

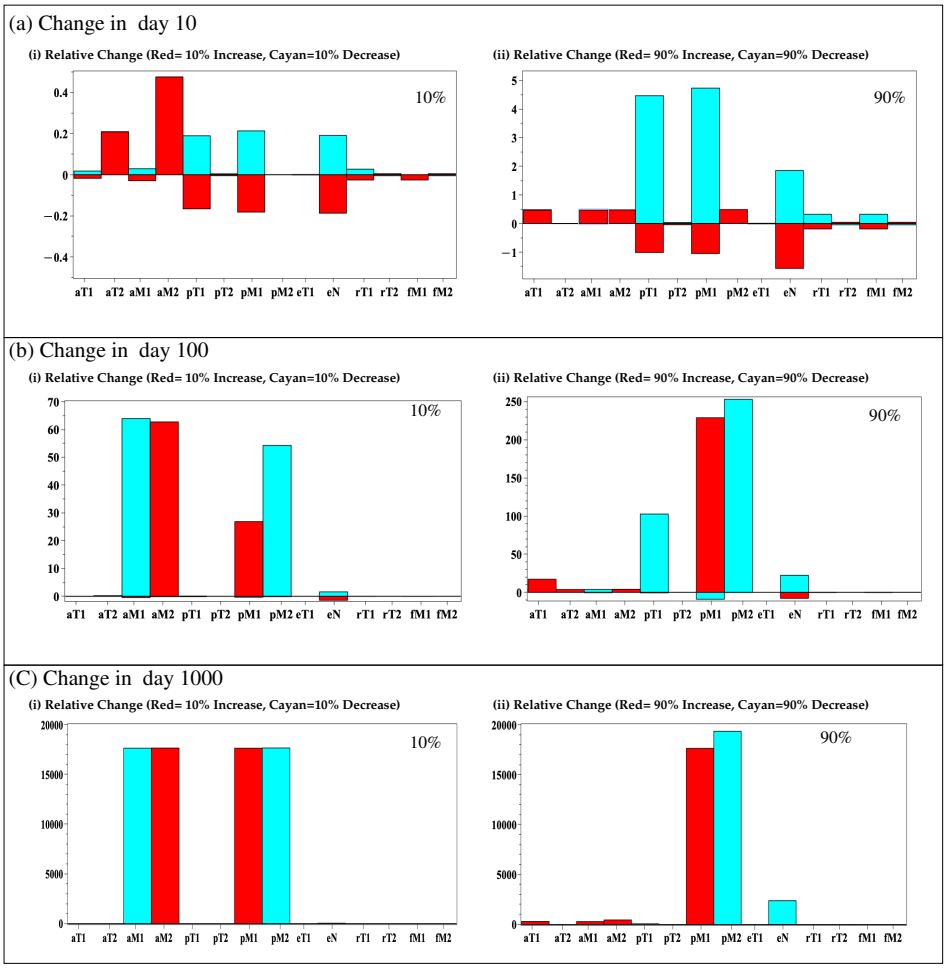

Figure 6: Sensitivity analysis of model (1) illustrating the impact of parameter variations on neuronal population dynamics. The analysis is performed at three time points: (a) day 10, (b) day 100, and (c) day 1000. A $\pm 10\%$ and $\pm 90\%$ perturbation is applied to each parameter relative to its baseline value. Red bars indicate parameters that positively influence neuronal population levels, while blue/cyan bars represent parameters that contribute to neuronal decline. The results highlight the relative importance of immune-related parameters in driving neuronal stability or degeneration over time. Baseline parameter values are provided in Table A.

ingly hostile to neurons, contributing to progressive neuronal deterioration and potential relapse of vulnerable neuronal populations.

Such mechanisms are consistent with clinical observations in neurodegenerative disorders, including Parkinson's disease, where elevated inflammatory markers and Th1-biased immune responses have been reported [13, 21]. Within the model, persistent inflammation gradually reduces the neuronal population, illustrating how an immune imbalance may drive neuronal relapse over time.

In contrast, when the immune response shifts toward Th2-associated pathways, microglia are more likely to adopt the M2 phenotype, which supports tissue repair and neuronal protection. Under these conditions, neuronal populations tend to stabilize, and

the harmful inflammatory cycle is attenuated. This suggests that restoring immune balance—either by reducing Th1 dominance or enhancing protective Th2 responses—may help prevent neuronal relapse and sustain neuronal stability. Such an interpretation is consistent with emerging therapeutic strategies that emphasize the role of IL-4 and other anti-inflammatory mediators in promoting neuroprotection [10].

The model therefore provides mechanistic insight into the processes driving the transition from neuronal stability to progressive neurodegeneration. The sensitivity analysis further demonstrates how delicate this balance is, as small perturbations in key immune-related parameters can significantly alter system outcomes. This highlights the importance of early intervention and identifies potential therapeutic targets aimed at preserving neuronal function.

Overall, the proposed model offers an integrated mathematical framework linking adaptive immune responses, microglial polarization, and neuronal stability. By capturing these interactions, the model suggests that immune imbalance is not merely a consequence of neurodegeneration but may actively drive relapse dynamics. These findings provide a theoretical basis for targeting key immune parameters to delay neuronal loss and enhance long-term neuronal resilience.

Future work may extend the present model to better represent the complex interactions between the immune system and the brain in neurodegenerative conditions, including Parkinson's disease. Incorporating additional immune components, such as natural killer (NK) cells, macrophages, and dendritic cells, could provide a more comprehensive description of how immune activity influences neuronal health. Further improvements may include modeling cytokine signaling in greater detail, including cytokine–receptor interactions and intracellular pathways, to better understand how immune signals propagate within the neural environment and affect neuronal survival. Integrating experimental or clinical data may also help refine parameter estimation and enhance the predictive capability of the model. Ultimately, this framework could be used to explore potential therapeutic strategies by simulating interventions that reduce excessive inflammation or promote protective immune responses, thereby helping to identify mechanisms that support neuronal survival and limit neuronal relapse.

More broadly, understanding how immune responses shape neuronal survival may open new opportunities for therapeutic strategies aimed at protecting vulnerable neuronal populations and slowing the progression of neurodegenerative disorders such as Parkinson's disease.

A. Parameter estimation

The parameter values used in model (1) are summarized in Table A. These values were selected based on a combination of previously reported data and calibrated estimates. Parameters linked to experimentally studied biological processes, such as immune cell interactions and microglial activation, were taken from the literature. For parameters without direct experimental measurements, values were chosen within biologically reasonable ranges to ensure that the model reflects realistic system behavior.

The calibration process involved restricting parameters to ranges reported in the literature and adjusting them to reproduce key features of neuroinflammatory dynamics. In particular, the model was tuned to capture the balance between pro-inflammatory (Th1/M1) and anti-inflammatory (Th2/M2) responses, the transition between neuronal stability and degeneration, and the emergence of threshold behavior driven by immune switching.

Parameter selection was guided by both biological relevance and the ability of the model to reproduce consistent dynamical behavior. Only parameter sets that preserved essential system properties—such as a stable, healthy state and a relapse regime under immune imbalance—were retained.

Sensitivity analysis was then used to examine how variations in parameters influence system behavior and to identify those with the strongest impact on neuronal outcomes. The analysis shows that the system is particularly sensitive to the transition rates r_{T1} and r_{T2}, which play a central role in controlling switching dynamics and threshold formation. Other parameters mainly affect the magnitude of responses without altering the overall qualitative behavior of the system.

Although not all parameters can be uniquely determined due to limited experimental data, the main mechanisms and qualitative predictions of the model remain stable under parameter variation. This indicates that the model captures the essential system dynamics, even without precise estimation of every individual parameter.

Such an approach is common in mathematical biology, where the focus is placed on understanding dominant mechanisms rather than obtaining exact parameter values.ion.

Param.	Description	Value	Units	Ref
a_{T1}	Th1 cell growth rate via M1 microglia	0.01–0.001	day^{-1} cell^{-1}	Estimation
a_{T2}	Th2 cell growth rate via M2 microglia	0.01–0.001	$\text{day}^{-1}\text{cell}^{-1}$	Estimation
a_{M1}	M1 microglia growth rate via Th1 cells	0.01–0.001	day^{-1}	Estimation
a_{M2}	M2 microglia growth rate via Th2 cells	0.01–0.001	day^{-1}	Estimation
β_T	Carrying capacity of Th cells	10000	cell	[36]
β_M	Carrying capacity of microglial cells	6000–12000 (8000)	cell	[37]
β_N	Carrying capacity of neuronal cells	8000–12000 (12000)	cell	[38]
e_{T1}	Th1 cell decay rate	0.035–0.069 (0.035)	day^{-1}	[39, 40]
e_{T2}	Th2 cell decay rate	0.2–0.05 (0.03)	day^{-1}	Estimation
e_{M1}	Decay rate of M1 microglial cells	0.0073	day^{-1}	[41, 42]
e_{M2}	Decay rate of M2 microglial cells	0.0073	day^{-1}	[41, 42]
e_N	Decay rate of neuronal cells	0.00001–0.001 (0.0007)	day^{-1}	Estimation
p_{T1}	Proliferation rate of Th1 cells via M1 microglia	0.01	$\text{day}^{-1}\text{cell}^{-1}$	Estimation
p_{T2}	Proliferation rate of Th2 cells via M2 microglia	0.01	$\text{day}^{-1}\text{cell}^{-1}$	Estimation
p_{M1}	Proliferation rate of M1 microglia via Th1 cells	0.02	$\text{day}^{-1}\text{cell}^{-1}$	Estimation
p_{M2}	Proliferation rate of M2 microglia via Th2 cells	0.02	$\text{day}^{-1}\text{cell}^{-1}$	Estimation
p_N	Activation rate of neuronal cells	0.1–5	day^{-1}	Estimation
r_{T2}	Rate of transition from Th1 to Th2	0.001–0.1	day^{-1}	Estimation
r_{T1}	Rate of transition from Th2 to Th1	0.001–0.1	day^{-1}	Estimation
f_{M1}	Elimination rate of neuronal cells by M1 microglia	10^{-5}–10^{-10}	$\text{day}^{-1}\text{cell}^{-1}$	Estimation
f_{M2}	Protection rate of neuronal cells by M2 microglia	10^{-5}–10^{-10}	$\text{day}^{-1}\text{cell}^{-1}$	Estimation

Table 1: Table summarising the parameters that appear in model (1)

.

Estimation of the Rate

- (Microglial Turnover in Resting Conditions): Based on experimental data, microglia are long-lived cells that maintain their population through slow self-renewal in the

healthy brain. Experimental studies estimate that their turnover occurs on the scale of several weeks to months [41, 42]. Assuming a representative half-life of approximately 95 days, the decay rate can be estimated as

$$t_{1/2} = 95 \text{ days}.$$

To compute the corresponding decay rate for modeling purposes, we apply the standard exponential decay formula:

$$\text{Decay rate} = \frac{\ln(2)}{t_{1/2}} = \frac{0.6931}{95} \approx 0.0073 \text{ day}^{-1}.$$

This result indicates that under normal, non-inflammatory conditions, approximately 0.73% of the microglial population is replaced or cleared each day.

- (Estimation of Th1 Cell Clearance Rate): A characteristic feature of classical Experimental Autoimmune Encephalomyelitis (EAE) models is that activated Th1 cells infiltrate the central nervous system (CNS) shortly after immunization, with disease onset typically occurring between days 10 and 20 [39, 40]. Following the peak inflammatory phase, the number of infiltrating T cells gradually declines as the immune response resolves.

  To represent this decline mathematically, we assume an exponential clearance process for Th1 cells. Since experimental studies indicate that activated T cells persist in the CNS for several days to weeks during the inflammatory response, we assume a representative half-life in the range of 10–20 days.

$$\text{Decay rate} = \frac{\ln(2)}{t_{1/2}},$$

  We obtain the following range:

$$\frac{\ln(2)}{10} \approx 0.069\,\text{day}^{-1}, \qquad \frac{\ln(2)}{20} \approx 0.035\,\text{day}^{-1}.$$

  Thus, the estimated Th1 clearance rate e_{T1} falls within the interval:

$$e_{T1} \in [0.035,\ 0.069]\ \text{day}^{-1}.$$

B. Stability of steady states.

In the following, we briefly examine the stability of the four steady-state types introduced in Section 2. The Jacobian matrix corresponding to system (1) is given by:

$$J = \begin{pmatrix} c_{11} & c_{12} & c_{13} & c_{14} & c_{15} \\ c_{21} & c_{22} & c_{23} & c_{24} & c_{25} \\ c_{31} & c_{32} & c_{33} & c_{34} & c_{35} \\ c_{41} & c_{42} & c_{43} & c_{44} & c_{45} \\ c_{51} & c_{52} & c_{53} & c_{54} & c_{55} \end{pmatrix} \tag{8}$$

where:

$$\begin{aligned}
c_{11} &= p_{T1}M1\left(1-\tfrac{2T1+T2}{\beta_T}\right) - e_{T1} - r_{T2} + a_{T1}M1 \\
c_{12} &= -\tfrac{p_{T1}T1M1}{\beta_T} + r_{T1} \\
c_{13} &= p_{T1}T1\left(1-\tfrac{T1+T2}{\beta_T}\right) + a_{T1}T1 \\
c_{14} &= 0 \\
c_{15} &= 0 \\
c_{21} &= -\tfrac{p_{T2}T_2M_2}{\beta_T} + r_{T2} \\
c_{22} &= p_{T2}M2\left(1-\tfrac{T1+2T2}{\beta_T}\right) - e_{T2} - r_{T1} + a_{T2}M2 \\
c_{23} &= 0 \\
c_{24} &= p_{T2}T2\left(1-\tfrac{T1+T2}{\beta_T}\right) + a_{T2}T2 \\
c_{25} &= 0 \\
c_{31} &= p_{M1}M1\left(1-\tfrac{M1+M2}{\beta_M}\right) + a_{M1}M1 \\
c_{32} &= 0 \\
c_{33} &= p_{M1}T1\left(1-\tfrac{2M1+M2}{\beta_M}\right) - e_{M1} + a_{M1}T1 \\
c_{34} &= -\tfrac{p_{M1}T1M1}{\beta_M} \\
c_{35} &= 0 \\
c_{41} &= 0 \\
c_{42} &= p_{M2}M2\left(1-\tfrac{M1+M2}{\beta_M}\right) + a_{M2}M2 \\
c_{43} &= -\tfrac{p_{M2}T2M_2}{\beta_M} \\
c_{44} &= p_{M2}T2\left(1-\tfrac{M1+2M2}{\beta_M}\right) - e_{M2} + a_{M2}T2 \\
c_{45} &= 0 \\
c_{51} &= 0 \\
c_{52} &= 0 \\
c_{53} &= -f_{M1}N \\
c_{54} &= f_{M2}N \\
c_{55} &= p_N\left(1-\tfrac{2N}{\beta_N}\right) - e_N + f_{M2}M2 - f_{M1}M1
\end{aligned}$$

Proposition 1. *The trivial equilibrium $E_0 = (0, 0, 0, 0, 0)$ is locally asymptotically stable if*

$$p_N < e_N.$$

Moreover, E_0 is unstable if

$$p_N > e_N.$$

Proof.
The Jacobian matrix associated with system (1) is

$$J = \begin{pmatrix} c_{11} & c_{12} & c_{13} & c_{14} & c_{15} \\ c_{21} & c_{22} & c_{23} & c_{24} & c_{25} \\ c_{31} & c_{32} & c_{33} & c_{34} & c_{35} \\ c_{41} & c_{42} & c_{43} & c_{44} & c_{45} \\ c_{51} & c_{52} & c_{53} & c_{54} & c_{55} \end{pmatrix}.$$

Evaluating J at the trivial equilibrium $E_0 = (0, 0, 0, 0, 0)$ gives

$$J(E_0) = \begin{pmatrix} -(e_{T1} + r_{T2}) & r_{T1} & 0 & 0 & 0 \\ r_{T2} & -(e_{T2} + r_{T1}) & 0 & 0 & 0 \\ 0 & 0 & -e_{M1} & 0 & 0 \\ 0 & 0 & 0 & -e_{M2} & 0 \\ 0 & 0 & 0 & 0 & p_N - e_N \end{pmatrix}.$$

Hence, the characteristic polynomial is

$$\det(\lambda I - J(E_0)) = (\lambda + e_{M1})(\lambda + e_{M2})(\lambda - (p_N - e_N))\Big[(\lambda + e_{T1} + r_{T2})(\lambda + e_{T2} + r_{T1}) - r_{T1} r_{T2}\Big].$$

After simplification, we obtain

$$\det(\lambda I - J(E_0)) = (\lambda + e_{M1})(\lambda + e_{M2})(\lambda - (p_N - e_N))\Big[\lambda^2 + (e_{T1} + e_{T2} + r_{T1} + r_{T2})\lambda + e_{T1} e_{T2} + e_{T1} r_{T1} + e_{T2} r_{T2}\Big].$$

Therefore, two eigenvalues are immediately

$$\lambda_1 = -e_{M1}, \qquad \lambda_2 = -e_{M2},$$

which are negative. The remaining two eigenvalues are roots of

$$\lambda^2 + (e_{T1} + e_{T2} + r_{T1} + r_{T2})\lambda + e_{T1} e_{T2} + e_{T1} r_{T1} + e_{T2} r_{T2} = 0.$$

Since all coefficients are positive, both roots have negative real parts. The last eigenvalue is

$$\lambda_5 = p_N - e_N.$$

It follows that all eigenvalues of $J(E_0)$ have negative real parts if and only if

$$p_N - e_N < 0,$$

that is,

$$p_N < e_N.$$

Hence, E_0 is locally asymptotically stable if $p_N < e_N$.

On the other hand, if

$$p_N > e_N,$$

then $\lambda_5 = p_N - e_N > 0$, and therefore E_0 is unstable.

C. Positive, bounded, and global solutions

Proposition 2. *For any non-negative initial data*

$$(T1(0), T2(0), M1(0), M2(0), N(0)) \in \mathbb{R}^5_+,$$

system (1) admits a unique solution

$$(T1(t), T2(t), M1(t), M2(t), N(t))$$

defined for all $t > 0$. Moreover, this solution remains non-negative and bounded in $\mathbb{R}^5_+$.

Proof.

(Local existence and uniqueness) Let

$$X = (T1, T2, M1, M2, N)^T,$$

and rewrite system (1) in the vector form

$$\frac{dX}{dt} = F(X), \qquad X(0) = X_0 \in \mathbb{R}^5_+.$$

Since each component of F is a polynomial function of the variables, F is continuously differentiable in $\mathbb{R}^5$. Hence, F is locally Lipschitz continuous on $\mathbb{R}^5$. By the Picard–Lindelöf theorem, there exists a unique local solution on some interval $[0, t_{\max})$.

(Positivity) Assume that $T1(0), T2(0), M1(0), M2(0), N(0) \geq 0$. From system (1), we have

$$\frac{dT1}{dt} \geq -(e_{T1} + r_{T2})T1,$$

which yields

$$T1(t) \geq T1(0) \exp\big(-(e_{T1} + r_{T2})t\big) \geq 0.$$

Similarly,

$$\frac{dT2}{dt} \geq -(e_{T2} + r_{T1})T2 \quad \Longrightarrow \quad T2(t) \geq T2(0) \exp\big(-(e_{T2} + r_{T1})t\big) \geq 0,$$

$$\frac{dM1}{dt} \geq -e_{M1}M1 \quad \Longrightarrow \quad M1(t) \geq M1(0)e^{-e_{M1}t} \geq 0,$$

$$\frac{dM2}{dt} \geq -e_{M2}M2 \quad \Longrightarrow \quad M2(t) \geq M2(0)e^{-e_{M2}t} \geq 0.$$

Also,

$$\frac{dN}{dt} \geq -(e_N + f_{M1}M1)N,$$

and therefore

$$N(t) \geq 0.$$

Thus, the non-negative orthant $\mathbb{R}^5_+$ is positively invariant.

(Boundedness) Assume that all initial data are nonnegative. Define

$$X(t) = T1(t) + T2(t), \qquad Y(t) = M1(t) + M_2(t).$$

We first derive an upper bound for $X(t)$. Using system (1), we have

$$\begin{aligned}\frac{dX}{dt} &= \frac{dT1}{dt} + \frac{dT2}{dt} \\ &= p_{T1}T1M1\left(1 - \frac{T1+T2}{\beta_T}\right) + a_{T1}T1M1 - e_{T1}T1 - r_{T2}T1 + r_{T1}T2 \\ &\quad + p_{T2}T2M2\left(1 - \frac{T1+T2}{\beta_T}\right) + a_{T2}T2M2 - e_{T2}T2 + r_{T2}T1 - r_{T1}T2.\end{aligned}$$

The transition terms cancel, so

$$\frac{dX}{dt} = T1M_1\left[p_{T1}\left(1 - \frac{X}{\beta_T}\right) + a_{T1}\right] + T2M2\left[p_{T2}\left(1 - \frac{X}{\beta_T}\right) + a_{T2}\right] - e_{T1}T1 - e_{T2}T2.$$

Now define

$$L_T = \max\left\{\beta_T\left(1 + \frac{a_{T1}}{p_{T1}}\right), \beta_T\left(1 + \frac{a_{T2}}{p_{T2}}\right)\right\}.$$

If $X \geq L_T$, then

$$p_{T1}\left(1 - \frac{X}{\beta_T}\right) + a_{T1} \leq 0, \qquad p_{T2}\left(1 - \frac{X}{\beta_T}\right) + a_{T2} \leq 0.$$

Hence, for $X \geq L_T$,

$$\frac{dX}{dt} \leq -e_{T1}T1 - e_{T2}T2 \leq 0.$$

Therefore, by the standard barrier argument,

$$X(t) \leq K_T := \max\{X(0), L_T\}, \qquad t \geq 0.$$

Next, we estimate $Y(t) = M1 + M2$. From system (1),

$$\begin{aligned}\frac{dY}{dt} &= \frac{dM1}{dt} + \frac{dM2}{dt} \\ &= p_{M1}T1M_1\left(1 - \frac{M1+M2}{\beta_M}\right) + a_{M1}T1M_1 - e_{M1}M1 \\ &\quad + p_{M2}T2M2\left(1 - \frac{M1+M2}{\beta_M}\right) + a_{M2}T2M2 - e_{M2}M2.\end{aligned}$$

Thus,

$$\frac{dY}{dt} = T1M_1 \left[p_{M1} \left(1 - \frac{Y}{\beta_M} \right) + a_{M1} \right] + T2M2 \left[p_{M2} \left(1 - \frac{Y}{\beta_M} \right) + a_{M2} \right] - e_{M1} M1 - e_{M2} M2.$$

Set

$$L_M = \max \left\{ \beta_M \left(1 + \frac{a_{M1}}{p_{M1}} \right), \beta_M \left(1 + \frac{a_{M2}}{p_{M2}} \right) \right\}.$$

If $Y \geq L_M$, then

$$p_{M1} \left(1 - \frac{Y}{\beta_M} \right) + a_{M1} \leq 0, \qquad p_{M2} \left(1 - \frac{Y}{\beta_M} \right) + a_{M2} \leq 0,$$

and therefore

$$\frac{dY}{dt} \leq -e_{M1} M1 - e_{M2} M2 \leq 0.$$

Hence,

$$Y(t) \leq K_M := \max\{Y(0), L_M\}, \qquad t \geq 0.$$

Finally, we study the neuronal population $N(t)$. From the fifth equation,

$$\frac{dN}{dt} = p_N N \left(1 - \frac{N}{\beta_N} \right) - e_N N + f_{M2} M_2 N - f_{M1} M1 N.$$

Since all variables are nonnegative, we have

$$-f_{M1} M1 N \leq 0, \qquad M2(t) \leq Y(t) \leq K_M.$$

Thus,

$$\frac{dN}{dt} \leq p_N N \left(1 - \frac{N}{\beta_N} \right) - e_N N + f_{M2} K_M N.$$

Equivalently,

$$\frac{dN}{dt} \leq (p_N - e_N + f_{M2} K_M) N - \frac{p_N}{\beta_N} N^2.$$

This is a logistic-type differential inequality. By comparison, $N(t)$ is bounded for all $t \geq 0$. In particular,

$$N(t) \leq K_N$$

for some positive constant K_N depending on the parameters and the initial value $N(0)$.

Combining the above estimates, we conclude that

$$T1(t) + T2(t) \leq K_T, \qquad M1(t) + M2(t) \leq K_M, \qquad N(t) \leq K_N,$$

for all $t \geq 0$. Therefore, every component $T1, T2, M1, M2, N$ is bounded on $[0, \infty)$. Consequently, the set

$$\Omega = \left\{ (T1, T2, M1, M2, N) \in \mathbb{R}^5_+ : T1 + T2 \leq K_T,\ M1 + M2 \leq K_M,\ N \leq K_N \right\}$$

is positively invariant and absorbing.

Funding

This research received no external funding.

Data Availability Statement

No datasets were generated or analyzed during the current study.

Conflict of Interest

The author declares no conflict of interest.

References

[1] S.Mullin and A.Schapira. α-synuclein and mitochondrial dysfunction in parkinson's disease. *Molecular neurobiology*, 47(2):587–597, 2013.

[2] M.Zaltieri, F.Longhena, M.Pizzi, C.Missale, P.Spano, and A.Bellucci. Mitochondrial dysfunction and α-synuclein synaptic pathology in parkinson's disease: Who's on first? *Parkinson's disease*, 2015(1):108029, 2015.

[3] A.Esteves, D.Arduino, D.Silvaand C.Oliveira, and S.Cardoso. Mitochondrial dysfunction: the road to alpha-synuclein oligomerization in pd. *Parkinson's disease*, 2011(1):693761, 2011.

[4] E.Srinivasan, G.Chandrasekhar, P.Chandrasekar, K.Anbarasu, A.Vickram, R.Karunakaran, R.Rajasekaran, and P.Srikumar. Alpha-synuclein aggregation in parkinson's disease. *Frontiers in medicine*, 8:736978, 2021.

[5] H.González, D.Elgueta, A.Montoya, and R.Pacheco. Neuroimmune regulation of microglial activity involved in neuroinflammation and neurodegenerative diseases. *Journal of neuroimmunology*, 274(1-2):1–13, 2014.

[6] H.González and R.Pacheco. T-cell-mediated regulation of neuroinflammation involved in neurodegenerative diseases. *Journal of neuroinflammation*, 11:1–11, 2014.

[7] M.Tansey, R.Wallings, M.Houser, M.Herrick, C.Keating, and V.Joers. Inflammation and immune dysfunction in parkinson disease. *Nature Reviews Immunology*, 22(11):657–673, 2022.

[8] Y.Zheng, Z.Ren, Y.Liu, J.Yan, C.Chen, Y.He, Y.Shi, F.Cheng, Q.Wang, C.Li, et al. T cell interactions with microglia in immune-inflammatory processes of ischemic stroke. *Neural Regeneration Research*, 20(5):1277–1292, 2025.

[9] R.Lisak, L.Nedelkoska, D.Studzinski, B.Bealmear, W.Xu, and J.Benjamins. Cytokines regulate neuronal gene expression: differential effects of th1, th2 and monocyte/macrophage cytokines. *Journal of Neuroimmunology*, 238(1-2):19–33, 2011.

[10] S.Subramaniam and H.Federoff. Targeting microglial activation states as a therapeutic avenue in parkinson's disease. *Frontiers in aging neuroscience*, 9:176, 2017.

[11] C.Depp, J.Doman, M.Hingerl, J.Xia, and B.Stevens. Microglia transcriptional states and their functional significance: Context drives diversity. *Immunity*, 58(5):1052–1067, 2025.

[12] Y.Chen, B.Qi, W.Xu, B.Ma, L.Li, Q.Chen, W.Qian, X.Liu, and H.Qu. Clinical correlation of peripheral cd4+-cell sub-sets, their imbalance and parkinson's disease. *Molecular Medicine Reports*, 12(4):6105–6111, 2015.

[13] N.Kustrimovic, C.Comi, L.Magistrelli, E.Rasini, M.Legnaro, R.Bombelli, I.Aleksic, F.Blandini, B.Minafra, G.Riboldazzi, et al. Parkinson's disease patients have a complex phenotypic and functional th1 bias: cross-sectional studies of cd4+ th1/th2/t17 and treg in drug-naïve and drug-treated patients. *Journal of neuroinflammation*, 15:1–17, 2018.

[14] G.Porenta and P.Riederer. A mathematical model of the dopaminergic synapse: stability and sensitivity analyses, and simulation of parkinson's disease and aging processes. *Cybernetics and System*, 13(3):257–274, 1982.

[15] A.Badrah and S.Al-Tuwairqi. Modeling the dynamics of innate immune response to parkinson disease with therapeutic approach. *Physical Biology*, 19(5):056004, 2022.

[16] S.Al-Tuwairqi and A. Badrah. Modeling the dynamics of innate and adaptive immune response to parkinson's disease with immunotherapy. *AIMS Mathematics*, 8(1):1800–1832, 2023.

[17] V.Belozyorov and V.Zaytsev. Mathematical modeling of parkinson's illness by chaotic dynamics methods. *Journal of Optimization, Differential Equations and Their Applications*, 25(8):21–39, 2017.

[18] M.Elfouly. Improved mathematical models of parkinson's disease with hopf bifurcation and huntington's disease with chaos. *Acta Biotheoretica*, 72(3):11, 2024.

[19] C.Baston, M.Contin, G.Calandra Buonaura, P.Cortelli, and M.Ursino. A mathematical model of levodopa medication effect on basal ganglia in parkinson's disease: an application to the alternate finger tapping task. *Frontiers in Human Neuroscience*, 10:280, 2016.

[20] U.Alon. *An Introduction to Systems Biology: Design Principles of Biological Circuits*. Chapman and Hall/CRC, 2006.

[21] W.Li, Y.Luo, H.Xu, Q.Ma, and Q.Yao. Imbalance between t helper 1 and regulatory t cells plays a detrimental role in experimental parkinson's disease in mice. *Journal of International Medical Research*, 49(4):0300060521998471, 2021.

[22] F.Aloisi, F.Ria, G.Penna, and L.Adorini. Microglia are more efficient than astrocytes in antigen processing and in th1 but not th2 cell activation. *The Journal of Immunology*, 160(10):4671–4680, 1998.

[23] M.Fishman and A.Perelson. Th1/th2 differentiation and cross-regulation. *Bulletin of mathematical biology*, 61(3):403–436, 1999.

[24] B.Morel, J.Kalagnanam, and P.Morel. Mathematical modeling of th1-th2 dynamics. In *Theoretical and experimental insights into immunology*, pages 171–190. Springer, 1992.

[25] X.Zhang, T.Brunner, L.Carter, R.Dutton, P.Rogers, L.Bradley, T.Sato, J. Reed, D.Green, and S.Swain. Unequal death in t helper cell (th) 1 and th2 effectors: Th1,

but not th2, effectors undergo rapid fas/fasl-mediated apoptosis. *The Journal of experimental medicine*, 185(10):1837–1849, 1997.

[26] G.Magombedze, S.Eda, and V.Ganusov. Competition for antigen between th1 and th2 responses determines the timing of the immune response switch during mycobaterium avium subspecies paratuberulosis infection in ruminants. *PLoS computational biology*, 10(1):e1003414, 2014.

[27] S.McCormick and N.Heller. Commentary: Il-4 and il-13 receptors and signaling. *Cytokine*, 75(1):38–50, 2015.

[28] J.Cherry and and M.O'Banion J.Olschowka. Neuroinflammation and m2 microglia: the good, the bad, and the inflamed. *Journal of neuroinflammation*, 11:1–15, 2014.

[29] D.Boche, V.Perry, and J.Nicoll. Activation patterns of microglia and their identification in the human brain. *Neuropathology and applied neurobiology*, 39(1):3–18, 2013.

[30] C.Prajeeth, K.Löhr, S.Floess, J.Zimmermann, R.Ulrich, V.Gudi, A.Beineke, W.Baumgärtner, M.Müller, J.Huehn, et al. Effector molecules released by th1 but not th17 cells drive an m1 response in microglia. *Brain, behavior, and immunity*, 37:248–259, 2014.

[31] L.Lawson, V.Perry, and S.Gordon. Turnover of resident microglia in the normal adult mouse brain. *Neuroscience*, 48(2):405–415, 1992.

[32] R.Franco and D.Fernández-Suárez. Alternatively activated microglia and macrophages in the central nervous system. *Progress in neurobiology*, 131:65–86, 2015.

[33] F.Gage. Neurogenesis in the adult brain. *Journal of neuroscience*, 22(3):612–613, 2002.

[34] E.Polazzi and A.Contestabile. Reciprocal interactions between microglia and neurons: from survival to neuropathology. *Reviews in the Neurosciences*, 13(3):221–242, 2002.

[35] B.Pettmann and C.Henderson. Neuronal cell death. *Neuron*, 20(4):633–647, 1998.

[36] V.Brochard, B.Combadière, A.Prigent, Y.Laouar, A.Perrin, V.Beray-Berthat, O.Bonduelle, D.Alvarez-Fischer, J. Callebert, J. Launay, et al. Infiltration of $cd4^+$ lymphocytes into the brain contributes to neurodegeneration in a mouse model of parkinson disease. *The Journal of clinical investigation*, 119(1), 2008.

[37] D.Sandra, M.Medeiros, J.Porfirio, et al. Similar microglial cell densities across brain structures and mammalian species: Implications for brain tissue function. *The Journal of Neuroscience*, 40(24):4622–4643, 2020.

[38] L.Brichta and P.Greengard. Molecular determinants of selective dopaminergic vulnerability in parkinson's disease: an update. *Frontiers in neuroanatomy*, 8:152, 2014.

[39] J.Goverman. Autoimmune t cell responses in the central nervous system. *Nature Reviews Immunology*, 9(6):393–407, 2009.

[40] L.Steinman. A molecular trio in relapse and remission in multiple sclerosis. *Nature Reviews Immunology*, 9(6):440–447, 2009.

[41] K.Askew, K.Li, A.Olmos-Alonso, F.Garcia-Moreno, Y.Liang, P.Richardson, T.Tipton, M.Chapman, K.Riecken, S.Beccari, et al. Coupled proliferation and apoptosis maintain the rapid turnover of microglia in the adult brain. *Cell reports*,

18(2):391–405, 2017.

[42] M.Bennett, F.Bennett, S.Liddelow, B.Ajami, J.Zamanian, N.Fernhoff, S.Mulinyawe, C.Bohlen, A.Adil, A.Tucker, et al. New tools for studying microglia in the mouse and human cns. *Proceedings of the National Academy of Sciences*, 113(12):E1738–E1746, 2016.